Reduced-Dimensional Quantum Approach to Tunneling Splittings Using Saddle-Point Normal Coordinates

Eugene Kamarchik, Yimin Wang, and Joel Bowman*

Cherry L. Emerson Center for Scientific Computation and Department of Chemistry, Emory University, Atlanta, Georgia 30322

Received: February 4, 2009; Revised Manuscript Received: March 3, 2009

We describe multidimensional extensions to a one-dimensional approach to tunneling splittings using a relaxed potential in the imaginary-frequency normal mode of the relevant saddle point (Wang, Y.; Bowman, J. M. *J. Chem. Phys.* **2008**, *129*, 121103). Tests of these extensions are given for H_3O^+ and NH_3 where full dimensional tunneling splittings are available and for the vinyl radical using a new full-dimensional potential energy surface.

I. Introduction

Hydrogen tunneling has long been recognized as playing an important role in a variety of chemical and biological processes. As a result, much effort has been directed toward the development of simple models that are hopefully able to accurately describe this phenomenon.[1,2] Beginning with Wigner in 1932,[3] a variety of model Hamiltonians for treating tunneling have been formulated. These models have, in turn, been applied to a number of molecules, notably malonaldehyde,[4−6] H_3O^+,[7,8] and ammonia[9] to elucidate factors that influence this behavior.

Given the difficulty of carrying out full-dimensional studies of most systems of interest, it is important to be able to identify the one (or a few) degree of freedom that is important to the tunneling process. Often this has involved the reduction of the $3N - 6$ degrees of freedom to a single degree of freedom. Perhaps the most widespread formulation of the approach is to identify the single degree of freedom as the intrinsic reaction coordinate (IRC) or, equivalently, as the minimum energy path (MEP).[10−13] This one coordinate is defined as the steepest descent path from a saddle-point transition state to the reactants and products. At the (first-order) saddle point that separates reactant and product states, there is a single imaginary frequency rectilinear normal mode, and in the Wigner theory the magnitude of this frequency determines the tunneling rate. The MEP theory can thus be regarded as a generalization of the Wigner method, which is meant to reduce the coupling along this coordinate and the remaining $3N - 7$ ones as the system proceeds from reactants to products via the corresponding saddle point.

The rigorous generalization of the IRC approach, referred to as the reaction path Hamiltonian, was given by Miller et al.[14] Given that the IRC is a curvilinear coordinate, the kinetic energy operator of this Hamiltonian is somewhat complex and approximations to it are often made (e.g., neglecting curvature terms). Recently, Rush and Wiberg[15] and Dong and Nesbitt[16,17] successfully applied an approximate version of the curvilinear Hougen−Bunker−Johns Hamiltonian[18] to calculations of tunneling splittings. (Rush and Wiberg's application was to ammonia and Dong and Nesbitt's applications were to H_3O^+ [16] and the vinyl radical.[17]) In the Rush−Wiberg implementation, an approximate but still curvilinear kinetic energy operator was used together with a one-dimensional relaxed potential in a large-amplitude coordinate (in their application, this was the "umbrella" angle) to define the 1D Hamiltonian. Dong and Nesbitt extended this approach by making the well-known vibrationally adiabatic (VA) approximation for the remaining $3N - 7$ degrees of freedom and adding the local vibrational energy to the relaxed potential. In these applications, the identity of the large amplitude coordinate is obvious; in the case of H_3O^+ and NH_3 it is the umbrella angle and for C_2H_3 it is the CCH bond angle.

We recently proposed another 1D approach to calculate tunneling processes.[19] In this approach, which can also be regarded as an extension of the Wigner method, the reaction coordinate is the imaginary-frequency normal mode Q_{im} of a saddle point separating reactants and products. The associated 1D Hamiltonian consists of a one-dimensional kinetic energy operator, neglecting the vibrational angular momentum (VAM) terms (also termed the Coriolis coupling terms), plus the potential in Q_{im} obtained by minimizing the full potential with respect to the remaining degrees of freedom for fixed values of Q_{im}. The VA approximation can also made in this 1D method; however, it was applied only for the zero-point energy in the other degrees of freedom. The method was tested for the tunneling splittings of malonaldehyde and d_1-malonaldehyde and the tunneling reaction probability for the $D + H_2$ reaction, for which exact full-dimensional results are available. The level of agreement was quite good, especially considering the simplicity (and generality) of the model.

The neglect of VAM terms in the normal-coordinate Watson Hamiltonian is one that is commonly made throughout the literature, and often it can be justified on the grounds that these terms scale like rotation constants, which are typically much smaller than vibrational term energies. For example, Viel et al. used the Watson Hamiltonian, neglecting the VAM terms, to calculate the tunneling splitting in malonaldehyde,[20] and Manthe and co-workers performed an almost exact calculation of the cumulative reaction probabilty for $H + CH_4$ using the same approximation.[21] Earlier, Seideman and Miller[22,23] used the exact Watson Hamiltonian to obtain the cumulative reaction probability, defined below, for the three-dimensional $H + H_2$ reaction using an exact method for zero total angular momentum, $J = 0$. They also demonstrated that neglecting the VAM terms in the Hamiltonian led to minor changes in the probability.[23]

* To whom correspondence should be addressed. E-mail: jmbowma@emory.edu.

10.1021/jp901027g CCC: $40.75
Published on Web 04/08/2009

Although 1D models can capture the basic behavior needed to describe tunneling, they can be improved by generalization to higher dimensions. Doing this using curvilinear coordinates, which provide a better zero-order description of large amplitude motion than rectilinear coordinates, requires the use of complex and coordinate-dependent kinetic energy operators. The approach taken here, which is based on using rectilinear coordinates, has the advantage of a universal kinetic energy operator, at least for nonlinear configurations. Extensions to include additional degrees of freedom go under the heading of reduced dimensional Hamiltonians and reaction surface Hamiltonians. Typically, the choice of the subset of degrees of freedom is made on the basis of physical grounds, often by first identifying so-called spectator degrees of freedom. An example is the $H_2 + CN \rightarrow HCN + H$, where CN is the spectator mode. A recent noteworthy example of such an approach is the reduced dimensionality approach taken by Sibert et al. to describe the double proton transfer in the formic acid dimer.[24,25] As stressed by that group, one advantage in considering more than one degree of freedom is the elimination of the vibrationally adiabatic approximation (for the coupled degrees of freedom), which, as they demonstrated and as is well known, can be problematic for excited states (due to avoided crossings, etc.). We base our choice of the set of coupled modes on the necessity of spanning the two minima, representing reactant and products, or two isomers and the associated saddle point separating them. Modes are added sequentially on the basis of the displacement they undergo in traversing these stationary points on the full-dimensional potential energy surface. The imaginary frequency mode Q_{im} is always included in the set of coupled modes. This generalization should increase the accuracy of the method by allowing for coupling among the large-amplitude modes. Another obvious advantage of a multidimensional theory is that convergence of results can be monitored with respect to the number of coupled modes, and that is a point emphasized here.

The details of the theory for this generalization are given in the next section. A simple approximation is also proposed to account for VAM coupling for the case of the 1D model. Following that, the computational methods used to obtain tunneling splittings for H_3O^+, NH_3, and the vinyl radical are described. Test results and discussion are then presented, followed by a summary and conclusions in the final section.

II. Theory

After a brief description of the Watson Hamiltonian, the simple one-dimensional case, where VAM terms are neglected, is reviewed, and its generalization to higher dimensions is given. In addition, a new one-dimensional model that includes approximate contributions from the VAM terms is presented. The computational algorithm that has been designed to implement this generalization is also described. All calculations here are for zero total angular momentum, J.

In terms of mass-scaled, rectilinear normal coordinates, the exact kinetic energy operator in atomic units for $J = 0$ is given by[26]

$$\hat{T} = \frac{1}{2}\sum_{\alpha\beta}\hat{\pi}_\alpha\mu_{\alpha\beta}\hat{\pi}_\beta - \frac{1}{8}\sum_{\alpha}\mu_{\alpha\alpha} - \frac{1}{2}\sum_{k}\frac{\partial^2}{\partial Q_k^2} \qquad (1)$$

where

$$\hat{\pi}_\alpha = -i\sum_{k,l}\zeta_{k,l}^{\alpha}Q_k\frac{\partial}{\partial Q_l} \qquad (2)$$

and $\mu_{\alpha\beta}$ is the inverse of the effective moment of inertia tensor and $\zeta_{k,l}^{\alpha}$ are the Coriolis coupling constants. The first term in this operator is known as the VAM term, while the second is the so-called "Watson" term, and the last is the standard kinetic energy operator in rectilinear coordinates.

A. Generalization of 1D Model without VAM. We will start with the generalization of the previously developed one-dimensional model to the multidimensional case. Neglecting the VAM terms and the "Watson" term yields the following simple Hamiltonian for the one-dimensional case

$$\hat{H} = -\frac{1}{2}\frac{\partial^2}{\partial Q_1^2} + V(Q_1) \qquad (3)$$

In general, we will take $Q_1 = Q_{im}$ so that the first mode is the one corresponding to the imaginary frequency at the saddle point. The potential, $V(Q_1)$, appearing in this Hamiltonian is fully relaxed with respect to the other degrees of freedom for a fixed value of Q_1. This Hamiltonian can be used in either one-dimensional calculations or approximate multidimensional ones such as the VA approximation. In this well-known approximation, the zero-point contributions of the remaining degrees of freedom are accounted for adiabatically. To implement this, a normal-mode analysis is done at the relaxed geometry corresponding to the minimum of the potential for a fixed Q_1, and the resulting frequencies are added to the potential. Within this approximation, the Hamiltonian becomes

$$\hat{H} = -\frac{1}{2}\frac{\partial^2}{\partial Q_1^2} + V_{VA}(Q_1) \qquad (4)$$

where

$$V_{VA}(Q_1) = V(Q_1) + \frac{1}{2}\sum_{k}^{3N-7}\omega_k(Q_1) \qquad (5)$$

The generalization to include multiple modes is straightforward. We will continue to use the notation that $Q_1 = Q_{im}$, and we will denote the second mode to be coupled as Q_2, the third mode as Q_3, and so on. Recall that unless specified otherwise the choice of these additional modes is based on the order of displacement of the modes from the saddle point to the minima. Again, starting from the Watson Hamiltonian and neglecting the VAM terms and the "Watson" term, we arrive at the Hamiltonian

$$\hat{H} = -\frac{1}{2}\sum_{i}^{M}\frac{\partial^2}{\partial Q_i^2} + V(Q_1,...,Q_M) \qquad (6)$$

where M is the total number of coupled modes, out of the $3N - 6$ modes, to be included in the calculation. The multidimensional potential, $V(Q_1,..., Q_M)$, is relaxed with respect to the remaining degrees of freedom for fixed values of $Q_1,..., Q_M$. The treatment of the remaining degrees of freedom can be formulated in several ways; we use the well-known adiabatic

approximation, which takes full advantage of relaxation. The relaxation can be performed using a variety of methods; here we used the standard generalized Newton method which requires the computation of the Hessian matrix. At convergence, the square root of the eigenvalues of the Hessian yields the frequencies, ω_k, at the relaxed geometry. Because this geometry is relaxed with respect to all remaining degrees of freedom, we are guaranteed that all ω_k's are real. At the transition state, these are simply the normal-mode frequencies corresponding to the transition-state normal modes; however, at other points, they correspond to the locally separable normal modes. Within this approximation, the uncoupled spectator modes are rotated to maintain their separability in response to the relaxed geometry determined by the fixed positions of the "active" modes. Using this approach and making the harmonic approximation results in the generalized Hamiltonian given by

$$\hat{H} = -\frac{1}{2}\sum_{i}^{M}\frac{\partial^2}{\partial Q_i^2} + V_{\mathrm{VA}}(Q_1,...,Q_M) \tag{7}$$

where

$$V_{\mathrm{VA}}(Q_1,...,Q_M) = V(Q_1,...,Q_M) + \frac{1}{2}\sum_{k}^{3N-6-M}\omega_k(Q_1,...,Q_M) \tag{8}$$

B. Model Including VAM Terms. There are cases (e.g., NH_3 and H_3O^+) where the VAM terms make a significant impact on the ground-state splitting, and therefore we also wish to develop an approximate treatment of these terms for the 1D model. The relaxed potential $V(Q_1)$ or $V_{\mathrm{VA}}(Q_1)$ defines a geometry on the potential energy surface $Q_{\mathrm{rel}}(Q_1) = \{Q_1, Q_2,..., Q_{3N-6}\}$. The inverse moment of inertia, $\mu_{\alpha\beta}$, is properly a function of all $3N - 6$ normal modes, and therefore we use the geometry provided by the relaxation $Q_{\mathrm{rel}}(Q_1)$. We can thus approximate the "Watson" term as

$$-\frac{1}{8}\sum_{\alpha}\mu_{\alpha\alpha}(Q_1,...,Q_{3N-6}) = -\frac{1}{8}\sum_{\alpha}\mu_{\alpha\alpha}[Q_{\mathrm{rel}}(Q_1)] \tag{9}$$

which makes it formally a function of only the single active mode. The normal-mode analysis at the relaxed geometry also provides a set of frequencies, ω_k, and eigenvectors, Q'_k, which are rotations of the original set of normal modes, for each fixed value of Q_1. By making the simple harmonic-oscillator approximation for each of these other degrees of freedom, we can represent the ground-state wave function for each by the corresponding ground-state harmonic-oscillator wave function

$$\psi(Q'_k) = \left(\frac{\omega_k}{\pi}\right)^{\frac{1}{4}}\exp\left(-\frac{\omega_k}{2}{Q'_k}^2\right) \tag{10}$$

and then averaging the VAM terms over these ground-state wave functions. This is consistent with making the VA approximation since the zero-point energy associated with this wave function is $\omega_k/2$. Evaluation of the VAM terms, $\Sigma_{\alpha\beta}\hat{\pi}_\alpha\mu_{\alpha\beta}\hat{\pi}_\beta$, then simply requires evaluation of the following well-known integrals for the ground-state harmonic oscillator wave functions:

$$\begin{aligned}
\int \psi^*(Q'_k)\frac{\partial^2}{\partial {Q'_k}^2}\psi(Q'_k)\,\mathrm{d}Q'_k &= -\frac{\omega_k}{2}\\
\int \psi^*(Q'_k)\frac{\partial}{\partial Q'_k}\psi(Q'_k)\,\mathrm{d}Q'_k &= 0\\
\int \psi^*(Q'_k){Q'_k}^2\psi(Q'_k)\,\mathrm{d}Q'_k &= \frac{1}{2\omega_k}\\
\int \psi^*(Q'_k)Q'_k\psi(Q'_k)\,\mathrm{d}Q'_k &= 0\\
\int \psi^*(Q'_k)Q'_k\frac{\partial}{\partial Q'_k}\psi(Q'_k)\,\mathrm{d}Q'_k &= -\frac{1}{2}\\
\int \psi^*(Q'_k)\frac{\partial}{\partial Q'_k}Q'_k\psi(Q'_k)\,\mathrm{d}Q'_k &= \frac{1}{2}
\end{aligned} \tag{11}$$

When we expand these terms, we get

$$-\frac{1}{2}\sum_{\alpha\beta}\sum_{i,j}\zeta_{i,j}^{\ \alpha}Q_i\frac{\partial}{\partial Q_j}\mu_{\alpha\beta}\sum_{k,l}\zeta_{k,l}^{\ \beta}Q_k\frac{\partial}{\partial Q_l} \tag{12}$$

and evaluating the integrals with respect to all the Q'_k modes, according to the equations in eq 11, yields the following expression for the one-dimensional VAM terms

$$\begin{aligned}
-\frac{1}{2}\sum_{\alpha\beta}\mu_{\alpha\beta}\Bigg[&\sum_{i,j}\zeta_{i,j}^{\ \alpha}\zeta_{i,j}^{\ \beta}\left(-\frac{\omega_j}{4\omega_i}-\frac{1}{4}\right)+\\
&\sum_{i}\zeta_{1,i}^{\ \alpha}\zeta_{1,i}^{\ \beta}\left(-{Q_1}^2\frac{\omega_i}{2}+\frac{1}{2\omega_i}\frac{\partial^2}{\partial {Q_1}^2}\right)+\\
&\zeta_{1,i}^{\ \alpha}\zeta_{i,1}^{\ \beta}\left(\frac{1}{2}\frac{\partial}{\partial Q_1}Q_1-\frac{1}{2}Q_1\frac{\partial}{\partial Q_1}\right)\Bigg]
\end{aligned} \tag{13}$$

We then add eqs 9 and 13 to our reference Hamiltonian in eq 4 to get a one-dimensional model that includes VAM. Because of the rotation of the original modes introduced by the use of the Q'_k modes, the coriolis coupling constants $\zeta_{i,j}^{\ \alpha}$ are themselves functions of Q_1, and therefore they must also be evaluated at each geometry defined by the choice of Q_1. The generalization of this approach to higher dimensions appears straightforward.

III. Computational Methods

To minimize the size of the basis needed to find eigenvalues and eigenfunctions of the Hamiltonian given by eq 7, we adopt the following scheme. First, an optimized set of grid points (described in detail below) is generated for each mode. Then the Hamiltonian corresponding to the two-dimensional subspace spanned by Q_1 and Q_2 in the grid basis is diagonalized and the eigenfunctions are saved. A subset of these eigenfunctions is then coupled with the grid basis for Q_3 to generate the three-dimensional subspace. Continuing in this fashion yields solutions to the four-, five-, and higher-dimensional Hamiltonians. Although the algorithm we implemented is completely general and can handle coupling an arbitrary number of modes, in practice six- or seven-dimensional calculations are the upper limit because of the increase in computational time with each additional mode.

We employ a discrete variable representation (DVR) basis[27,28] derived from the sinc function to represent each normal mode that will be included in the calculation. The integrals are approximated using the appropriate numerical quadrature.

Starting from the primitive one-particle basis,

$$\left\{\phi_i(Q) = \frac{\sin[\pi(Q - ih)/h]}{\pi(Q - ih)/h},\ i = -\frac{n_{\mathrm{DVR}}}{2},...,\frac{n_{\mathrm{DVR}}}{2}\right\} \quad (14)$$

yields an equally spaced grid of $n_{\mathrm{DVR}} + 1$ points over the interval $[-hn_{\mathrm{DVR}}, hn_{\mathrm{DVR}}]$. This interval can be shifted so that it is centered at any other location by a trivial change of variables. In this basis, the potential is diagonal and the kinetic energy operator is given as[29]

$$\langle\phi_i(Q)|\hat{T}|\phi_j(Q)\rangle = \begin{Bmatrix} -\dfrac{\pi^2}{3h^2} & i = j \\ (-1)^{|i-j|}\dfrac{2}{h^2(i-j)^2} & i \neq j \end{Bmatrix} \quad (15)$$

From an initially dense equally spaced grid, we can contract to a smaller set of basis functions, the potential optimized (PODVR) basis, by solving the equivalent reference Hamiltonians given by eq 4 for each mode. The eigenfunctions, $\psi(Q)$, corresponding to the lowest n_{PODVR} eigenvalues are taken and the matrix corresponding to the coordinate operator

$$X_{i,j} = \langle\psi_i(Q)|\hat{Q}|\psi_j(Q)\rangle \quad (16)$$

is constructed. Diagonalization of this matrix then yields a new set of n_{PODVR} grid points that are optimum for the Hamiltonian,[30,31] and which we will denote as $\phi_i^{\mathrm{PO}}(Q)$. To evaluate the matrix elements of the kinetic energy operator within the $\phi_i^{\mathrm{PO}}(Q)$ basis, the elements in the primitive basis, $\phi_i(Q)$, are first transformed using the eigenfunctions, $\psi(Q)$, of the reference Hamiltonian and then transformed again using the eigenfunctions of the coordinate operator to give, finally, $\langle\phi_i^{\mathrm{PO}}(Q|\hat{T}|\phi_j^{\mathrm{PO}}(Q)\rangle$.

Starting from the case where $M = 2$, we use the direct product basis

$$|\phi_{i,j}^{\mathrm{PO}}(Q_1, Q_2)\rangle = |\phi_i^{\mathrm{PO}}(Q_1)\rangle \cdot |\phi_j^{\mathrm{PO}}(Q_2)\rangle \quad (17)$$

of the PODVR grids in the first two modes. Equation 7 is then solved in this basis, and a set of eigenfunctions from this calculation is saved. The $M = 3$ equations are then solved in the direct product basis

$$|\phi_{i,j}(Q_1, Q_2, Q_3)\rangle = |\psi_i(Q_1, Q_2)\rangle \cdot |\phi_j^{\mathrm{PO}}(Q_3)\rangle \quad (18)$$

where $\psi_i(Q_1,Q_2)$ is an eigenfunction from the $M = 2$ calculation and $\phi_j^{\mathrm{PO}}(Q_3)$ is one of the PODVR functions in the third mode. This scheme can then be applied iteratively until the desired level of mode coupling is reached.

For the $M = 3$ equations, the kinetic energy matrix elements are

$$\langle\phi_{i,j}|\hat{T}|\phi_{k,l}\rangle = \delta_{j,l}\langle\psi_i|\ -\ \frac{1}{2}(\nabla_1^{\,2} + \nabla_2^{\,2})|\psi_k\rangle + \delta_{i,k}\langle\phi_j|\ -\ \frac{1}{2}(\nabla_3^{\,2})|\phi_l\rangle \quad (19)$$

The two terms here are, respectively, the transformation of the kinetic energy integrals from the previous calculation and the PODVR kinetic energy grid. The potential energy elements can be calculated as

$$\begin{aligned}\langle\phi_{i,j}|\hat{V}|\phi_{k,l}\rangle &= \int \psi_i(Q_1, Q_2)\phi_j(Q_3)V_{\mathrm{VA}}(Q_1, Q_2, Q_3)\ \times \\ &\quad \psi_k(Q_1, Q_2)\phi_l(Q_3)\,\mathrm{d}Q_1\,\mathrm{d}Q_2\,\mathrm{d}Q_3 = \\ &\int \sum_{i',j'} c_{i',j'}^{(i)}\phi_{i'}(Q_1)\phi_{j'}(Q_2)\phi_j(Q_3)V_{\mathrm{VA}}(Q_1, Q_2, Q_3)\ \times \\ &\quad \sum_{k',l'} c_{k',l'}^{(k)}\phi_{k'}(Q_1)\phi_{l'}(Q_2)\phi_l(Q_3)\,\mathrm{d}Q_1\,\mathrm{d}Q_2\,\mathrm{d}Q_3 = \\ &\delta_{j,l}\int \sum_{i',j'} c_{i',j'}^{(i)}\phi_{i'}(Q_1)\phi_{j'}(Q_2)V_{\mathrm{VA}}(Q_1, Q_2, Q_3^{\,j})\ \times \\ &\quad \sum_{k',l'} c_{k',l'}^{(k)}\phi_{k'}(Q_1)\phi_{l'}(Q_2)\,\mathrm{d}Q_1\,\mathrm{d}Q_2 = \\ &\quad \delta_{j,l}\sum_{i',j'} c_{i',j'}^{(i)}c_{i',j'}^{(k)}V_{\mathrm{VA}}(Q_1,^{i'}Q_2,^{j'}Q_3^{\,j}) \end{aligned} \quad (20)$$

where $Q_1^{\,i}$ represents the ith PODVR point for mode one, and we employed the fact that the potential is diagonal in the PODVR representation to arrive at the latter two expressions. Similar formulas can be written for the kinetic and potential matrix elements appearing in the $M = 4, 5,...$ equations.

The one-dimensional Hamiltonian including VAM terms is also solved using a sinc basis. Because we did not implement the higher-dimensional cases that would require a similar sequential subspace diagonalization and recoupling approach, no further computational details are provided for this method.

IV. Tests and Discussion

The reduced-dimensional approach to calculating vibrational splittings was tested on three molecules: the vinyl radical, H_3O^+, and ammonia, and the results are presented here. These tests are meant to illustrate the convergence of the generalization with respect to increasing number of coupled modes, the ability of the method to capture information about excited states, and the importance of including VAM terms in the one-dimensional model for H_3O^+ and NH_3.

A. Vinyl Radical. The vinyl radical possess a C_{2v} saddle-point transition state corresponding to a hydrogen migration between two equivalent C_s global minima. This hydrogen moves in a double well potential with a relatively low barrier and thus results in measurable tunneling splittings of the vibrational levels.[32,33] Various reduced dimensional calculations of the tunneling splittings of the vinyl radical were done using the approach described above. A new ab initio-based global potential energy surface (PES)[34] was used in these calculations. We use the criteria described above to pick the first three normal modes

TABLE 1: Nine Normal Modes, Their Frequencies, and Their Displacements at the Global Minimum for the Vinyl Radical

mode	frequency	displacement at global minimum
Q_1	654.7i	–56.9
Q_2	3380.6	–19.6
Q_3	929.9	–9.0
Q_4	3026.7	0.8
Q_5	582.1	0.0
Q_6	895.6	0.0
Q_7	1385.3	3.5
Q_8	1589.7	–3.7
Q_9	3085.4	–0.4

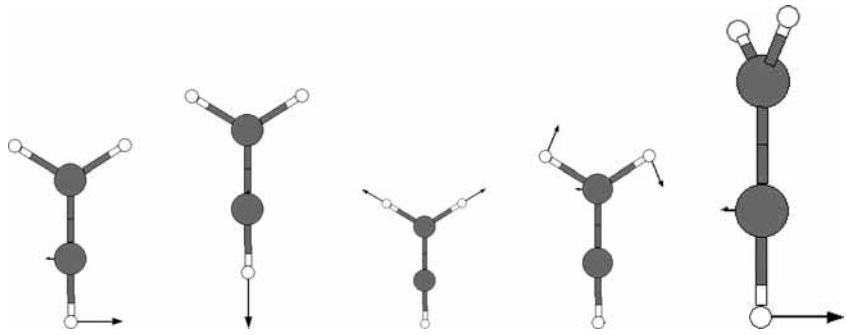

Figure 1. Five transition-state normal modes included in the vinyl calculation. From left they are Q_1, Q_2, Q_3, Q_4, and Q_5.

TABLE 2: Tunneling Splitting for Vinyl with Three Different Multidimensional Approaches[a]

modes used	no relaxation	relaxed potential	VA approximation
Q_1	271.65	0.60	0.51
Q_1,Q_2	0.62	0.34	0.48
Q_1,Q_2,Q_3	0.32	0.36	0.43
Q_1,Q_2,Q_3,Q_4	0.30	0.39	0.43
Q_1,Q_2,Q_3,Q_4,Q_5	0.43		

[a] All values are in units of wavenumbers. As the dimensionality of all three is increased, they approach 0.43 cm^{-1}. At low-dimensionality, the VA approximation delivers the best approximation to the exact answer.

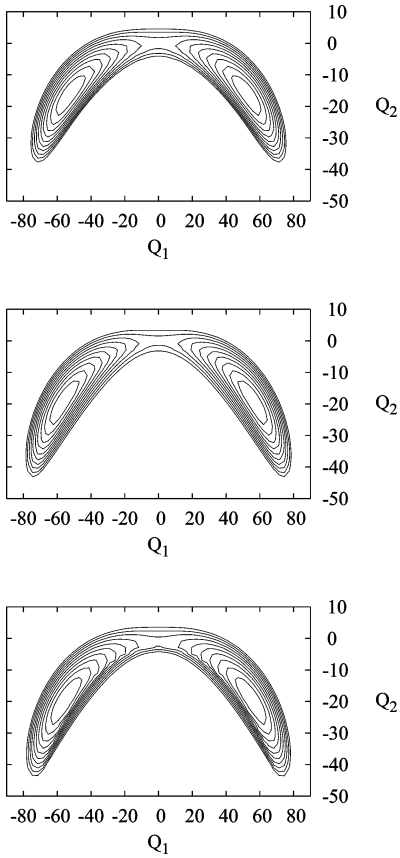

Figure 2. Contour plot for vinyl potential energy surface as a function of modes one and two. From top to bottom, these are the unrelaxed surface, the relaxed surface, and the relaxed surface in the vibrationally adiabatic approximation. Contour lines are spaced at intervals of 200 cm^{-1}, and the potentials are shifted so that the minimum for each is at 0.

(Q_1, Q_2, and Q_3) to be coupled. The fourth mode was chosen to permit comparison with recent experimental results of Dong et al.[33] of the tunneling splitting for the fundamental of that mode (the symmetric CH_2 stretch). A fifth mode, which corresponds to an out-of-plane motion, was added finally in one type of calculation; even so-called "spectrator" modes can have an influence on the tunneling splitting. A list of the saddle-point normal modes along with their frequencies and displacements at the global minimum are give in Table 1, and they are depicted in Figure 1.

All calculations were done neglecting the VAM terms, which we expect to be small (see below for further discussion of this). Calculations were done without relaxing the potential, with the relaxed potential but no VA treatment of the "spectrator" modes, and with the relaxed potential and including the ground-state VA approximation. The results for the ground-state tunneling splitting are given in Table 2. Consider first the results without a relaxed potential. As seen, the splitting changes significantly with the number of modes and for the largest five-mode calculation it is 0.43 cm^{-1}. It is significant that the inclusion of mode five affects the tunneling splitting significantly even though that mode is not displaced at the global minimum (cf., Table 1). The results for the relaxed potential without the VA approximation vary from 0.34 to 0.39 cm^{-1} as the number of coupled modes increases from two to four. Finally, the "preferred" VA results show very good stability of the splitting in going from two to four coupled modes, with a seemingly converged result of 0.43 cm^{-1}. While an exact result is not yet available on this PES, preliminary results using the MULTIMODE reaction path Hamiltonian approach[35] give a ground-state splitting of approximately 0.42 cm^{-1}, in excellent agreement with the VA result here. Since this approach does not neglect VAM terms, the agreement with the present calculations also validates the neglect of VAM terms in the present calculations. Also, it is worth noting that the calculated splitting is in good agreement with the experimental splitting of 0.514 cm^{-1}.[32]

The differences in splitting between the various calculations can, for the most part, be accounted for by differences in the barrier height of the associated potentials. This is seen most dramatically for the one-mode calculation, where the unrelaxed potential has a barrier of 270 cm^{-1}, which is much smaller than the barrier of the full-dimensional PES (and also the relaxed potential) of 1720 cm^{-1}. The splitting for the unrelaxed 1D potential is, as a result, very large (and very wrong). A much improved result for the splitting is seen for the relaxed potential and somewhat improved over that with the VA approximation. For the two-dimensional calculation, the unrelaxed potential has a barrier of 1200 cm^{-1} and with the VA approximation the effective barrier is 1550 cm^{-1}. Contour plots of the three different 2D potential surfaces generated by each of these methods are shown in Figure 2. It is worth noting the strong correlation between these two modes, as evidenced by the large curvature of the contour lines.

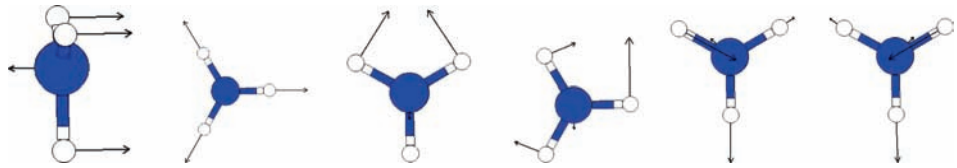

Figure 3. Six transition-state normal modes for ammonia. From left they are the umbrella mode Q_1, the symmetric stretch Q_2, the degenerate bends Q_3 and Q_4, and the degenerate stretches Q_5 and Q_6.

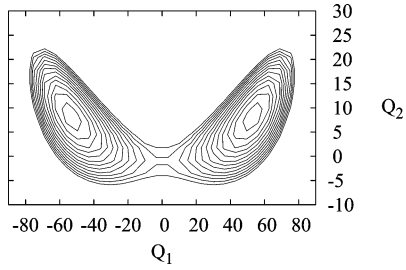

Figure 4. Contour plot for the relaxed ammonia potential energy surface in the vibrationally adiabatic approximation as a function of modes one and two. Contour lines are spaced at intervals of 200 cm^{-1}.

TABLE 3: Comparison of "Exact" Tunneling Splittings with One- and Two-Dimensional Calculations for Ammonia[a]

splitting	"exact"	1D	2D
gs	0.20	0.18	0.20
ν_1	11.12	12.73	12.36
$2\nu_1$	173.34	193.12	177.14
$3\nu_1$	460.72	497.71	461.47

[a] The ground state, denoted by gs, and the first few vibrational levels are compared. All values in are wavenumbers.

TABLE 4: Comparison of Exact Results with One- and Two-Dimensional Calculations on H_3O^+

splitting	"exact"	1D	2D
gs	21.94	19.00	22.48
ν_1	272.90	270.61	274.67
$2\nu_1$	600.64	549.69	527.57
ν_2	16.68		17.73

Clearly, as the number of coupled modes is increased the barrier of the unrelaxed potential gets closer to the correct value, and also the effect of the VA treatment of the spectrator modes decreases. Thus, the tunneling splitting also gets closer to the correct value. This is seen clearly by the results in Table 1. However, this approach clearly requires a significant number of modes in general, and since it does not contain any treatment of the "spectrator" modes it is not recommended.

The calculations with the relaxed potential, which has the correct barrier height, are, as expected, much more accurate than those with the unrelaxed potential. In the present example, it does appear that at least two modes are needed to get within roughly 20% of the correct result. Adding the VA approximation evidently is effective in achieving a satisfactory level of accuracy. Even for the one-mode calculation the splitting is 20% higher than the converged result and the two-mode calculation splitting is only 10% higher than the converged result. These are encouraging results for a problem with nine vibrational degrees of freedom.

As noted, another advantage of the reduced-dimensionality generalization is its ability to make predictions about the excited-state splittings for any mode included in the calculation by explicitly including the mode of interest in the group of coupled modes. In particular, for the vinyl radical, the recent experimental work of Dong et al. suggests that the splitting increases by roughly 0.07 cm^{-1} for the fundamental of the CH_2 symmetric stretch.[33] This is indeed consistent with the theoretical prediction within the present four-mode VA calculation where the splitting of this fundamental is 0.51 cm^{-1}, which is about 0.08 cm^{-1} larger than ground-state splitting.

B. Ammonia. As a second example, we consider the tunneling splittings of NH_3. Because ammonia has only six degrees of freedom, it was possible to use the iterative diagonalization/recoupling algorithm already presented to calculate the "exact" splitting, coupling all six modes. Note that we continue to neglect the VAM terms (which as we shall show are significant for NH_3), and thus we put quotes around exact. Although we used 30 PODVR points in each dimension and saved 60 eigenfunctions at each iterative step, there may still be variation on the order of 0.01 cm^{-1} in each result. For this study, we used the realistic potential energy surface of Léonard et al.,[9] which has an inversion barrier of 1820 cm^{-1}. (These authors also reported full-dimensional tunneling splittings and energies using this PES.)

The six normal modes at the transition state are illustrated in Figure 3, and we will use the notation that Q_1 is the umbrella motion, Q_2 corresponds to the symmetric stretch, Q_3 and Q_4 correspond to the degenerate bends, and Q_5 and Q_6 correspond to the degenerate stretches. Only two of the saddle-point normal modes, Q_1 and Q_2, are needed to span both the global minimum and the transition state, and therefore we expect the 2D results will give very good agreement with the "exact" results. (Note that our designation of normal modes differs from what is used in ref 9 and conforms to our convention of labeling the largest amplitude saddle-point mode by Q_1.) A contour plot of the 2D potential energy within the VA approximation is presented in Figure 4. Table 3 shows the comparison of the "exact" 6D result (neglecting VAM terms) with the corresponding reduced-dimensional results using the relaxed potential and the VA approximation.

The splittings for both the ground state and several excited states in the inversion mode are shown in Table 3. The 2D calculation shows very good agreement for the ground state and the first three excitations of Q_1 with the 6D results and even the 1D splittings are in good agreement with the "exact" ones.

The present "exact" ground-state splitting of 0.2 cm^{-1} is not in good agreement with the full-dimensional splitting,[9] which does not neglect the VAM terms, between 0.6 and 0.68 cm^{-1}. This clearly indicates that neglect of the VAM terms in ammonia is not a good approximation. This in not surprising given that the saddle point is of D_{3h} symmetry, and thus there are two sets of doubly degenerate saddle-point normal modes. We estimated the effect of the VAM using the present 1D model with VAM and found a ground-state splitting of 1.12 cm^{-1}, which certainly indicates a large effect.

C. H_3O^+. A molecule with much larger tunneling splittings than the two already considered is H_3O^+, which is similar in structure to ammonia. The normal modes and potential energy contours are similar to those for ammonia, and therefore they

are not repeated here. The PES used in the present calculations is the one developed by Huang et al.[7] (denoted HCB-3).

Even though, based on the results for NH_3, we anticipate significant effects from the VAM terms, we examined the accuracy of reduced dimensional calculations neglecting them. The modes chosen for the calculations were, in order, the umbrella mode, the symmetric stretch, and one of the degenerate bends. Table 4 shows the comparison of the six-dimensional result, neglecting VAM, with the reduced dimensional results. As seen, there is very good agreement for the ground-state splitting and excited inversion-mode splittings even with the 1D VA calculations. Results for the splittings corresponding to some other excited states are also given. For the fundamental of the symmetric stretch, Q_2, the 2D results are in very good agreement with the "exact" one.

The exact ground-state splitting (based on using the full Watson Hamiltonian) for the HCB-3 potential is 46 cm^{-1},[7] which is significantly larger than the present "exact" value of 21.9 cm^{-1}. The error in the present calculation is due to neglect of the VAM terms. The present 1D model to incorporate the VAM terms does yield a ground-state splitting of 50 cm^{-1}, which is a significant improvement over the result neglecting VAM terms.

V. Summary and Conclusions

The results presented here are encouraging for the development of reduced-dimensionality approaches to tunneling. The generalization of the one-dimensional approach allows the accuracy of the calculation to be increased in a systematic way and can predict splittings using two- or three-dimensional calculations with high accuracy. All three molecules demonstrate excellent agreement between the low-dimensional results and the exact results if VAM terms are neglected. Initial efforts to approximately include the VAM coupling were described using a 1D model, and it will be important to incorporate this coupling, when warranted, to the higher dimensional models.

This generalization offers several improvements over the one-dimensional method. As noted, several other authors demonstrated the multidimensional nature of tunneling[24,25,36,37] in a variety of important molecules, and therefore it is important to be able to effectively treat this issue. Also, as the dimensionality is increased, it will necessarily start to approach the exact result, since it must agree at full dimensionality. The choice of which additional modes to include can be made based on the necessity of spanning both the transition state and minimum, and the importance of modes can be estimated from the displacement in traversing these two locations. This method thus provides a systematic and general method for improving the accuracy of the 1D results.

Acknowledgment. We thank the Office of Naval Research (N000140710589) for financial support.

References and Notes

(1) Benderskii, V. A.; Makarov, D. E.; Wight, C. A. *Chemical Dynamics at Low Temperatures*; Advances in Chemical Physics 88; Wiley: New York, 1994.

(2) *Hydrogen-Transfer Reactions*; Schowen, R. L., Klinman, J. P., Hynes, J. T., Limbach, H. H., Eds.; Wiley-VCH: Weinheim, Germany, 2007.

(3) Wigner, E. *Z. Phys. Chem. Abt. B* **1932**, *19*, 203.

(4) Wang, Y.; Braams, B. J.; Bowman, J. M.; Carter, S.; Tew, D. P. *J. Chem. Phys.* **2008**, *128*, 224314.

(5) Tew, D. P.; Handy, N. C.; Carter, S. *J. Chem. Phys.* **2006**, *125*, 084313.

(6) Mil'nikov, G. V.; Yagi, K.; Taketsugu, T.; Nakamura, H.; Hirao, K. *J. Chem. Phys.* **2004**, *120*, 5036.

(7) Huang, X.; Carter, S.; Bowman, J. *J. Chem. Phys.* **2003**, *118*, 5431.

(8) Miani, A.; Beddoni, A.; Pesonen, J.; Halonen, L. *Chem. Phys. Lett.* **2002**, *363*, 52.

(9) Léonard, C.; Handy, N.; Carter, S.; Bowman, J. *Spectrochim. Acta* **2002**, *58*, 825.

(10) Marcus, R. *J. Chem. Phys.* **1965**, *43*, 1598.

(11) Hofacker, L. *Z. Naturforsch.* **1965**, *43*, 1598.

(12) Fukui, K. *J. Phys. Chem.* **1970**, *74*, 4161.

(13) Ishida, K.; Morokuma, K.; Komornicki, A. *J. Chem. Phys.* **1977**, *66*, 2153.

(14) Miller, W. H.; Handy, N. C.; Adams, J. E. *J. Chem. Phys.* **1980**, *72*, 99.

(15) Rush, F. J.; Wiberg, K. *J. Phys. Chem. A* **1997**, *101*, 3143.

(16) Dong, F.; Nesbitt, D. J. *J. Chem. Phys.* **2006**, *125*, 144311.

(17) Nesbitt, D. J.; Dong, F. *Phys. Chem. Chem. Phys.* **2008**, *10*, 2113.

(18) Hougen, J. T.; Bunker, P. R.; Johns, J. W. C. *J. Mol. Spectrosc.* **1970**, *34*, 136.

(19) Wang, Y.; Bowman, J. M. *J. Chem. Phys.* **2008**, *129*, 121103.

(20) Viel, A.; Coutinho-Neto, M. D.; Manthe, U. *J. Chem. Phys.* **2007**, *126*, 024308.

(21) Wu, T.; Werner, H.-J.; Manthe, U. *J. Chem. Phys.* **2006**, *124*, 164307.

(22) Seideman, T.; Miller, W. H. *J. Chem. Phys.* **1992**, *96*, 4412.

(23) Seideman, T.; Miller, W. H. *J. Chem. Phys.* **1992**, *97*, 2499.

(24) Barnes, G. L.; Sibert, E. L. *J. Chem. Phys.* **2008**, *129*, 164317.

(25) Barnes, G. L.; Squires, S. M.; Sibert, E. L. *J. Phys. Chem. B* **2008**, *112*, 595.

(26) Watson, J. K. G. *Mol. Phys.* **1968**, *15*, 479.

(27) Dickinson, A. S.; Certain, P. R. *J. Chem. Phys.* **1968**, *49*, 4209.

(28) Light, J.; Carrington, T. In *Advances in Chemical Physics*; Prigogine, I., Rice, S. A., Eds.; Wiley: New York, 2000; Vol. 114, pp 263−310.

(29) Boyd, J. P. *Chebyshev and Fourier Spectral Methods*, 2nd ed.; Dover Publications: Mineola, NY, 2001.

(30) Harris, D. O.; Engerholm, G. G.; Gwinn, W. D. *J. Chem. Phys.* **1965**, *43*, 1515.

(31) Echave, J.; Clary, D. C. *Chem. Phys. Lett.* **1992**, *190*, 225.

(32) Tanaka, K.; Toshimitsu, M.; Harada, K.; Tanaka, T. *J. Chem. Phys.* **2004**, *120*, 3604.

(33) Dong, F.; Roberts, M.; Nesbitt, D. J. *J. Chem. Phys.* **2008**, *128*, 044305.

(34) Sharma, A.; Braams, B.; Carter, S.; Shepler, B. C.; Bowman, J. M. *J. Chem. Phys.*, in press.

(35) Carter, S.; Handy, N. *J. Chem. Phys.* **2000**, *113*, 987.

(36) Paz, J. J.; Moreno, M.; Lluch, J. M. *J. Chem. Phys.* **1995**, *103*, 353.

(37) Bosch, E.; Moreno, M.; Lluch, J. M.; Bertrán, J. *J. Chem. Phys.* **1990**, *93*, 5685.

JP901027G